Energy, exergy, sustainability and economic analysis of waste tire pyrolysis oil blends with different nanoparticle additives in spark ignition engine

Haseeb Yaqoob[1,2], Yew Heng Teoh[1,♣], Farooq Sher[3], Muhammad Ahmad Jamil[4], Mubbashar Ali[2], Ümit Ağbulut[5,†], Hamza Ahmad Salam[2], Muhammad Arslan[2], Manzoore Elahi M. Soudagar[6], M.A. Mujtaba[7], Ashraf Elfasakhany[8], Asif Afzal[9]

[1] School of Mechanical Engineering, Universiti Sains Malaysia, Engineering Campus, 14300 Nibong Tebal, Penang, Malaysia.

[2] Department of Mechanical Engineering, Khwaja Fareed University of Engineering and Information Technology, Rahim Yar Khan 64200, Pakistan.

[3] Department of Engineering, School of Science and Technology, Nottingham Trent University, Nottingham NG11 8NS, UK.

[4] Department of Mechanical and Construction Engineering, Northumbria University, Newcastle Upon Tyne NE1 8ST, UK.

[5] Department of Mechanical Engineering, Faculty of Engineering, Düzce Uniersity, 81620, Düzce, Turkey.

[6] Department of Mechanical Engineering, School of Technology, Glocal University, Delhi-Yamunotri Marg, SH-57, Mirzapur Pole, Saharanpur District, Uttar Pradesh 247121, India.

[7] Department of Mechanical Engineering, University of Engineering and Technology, New Campus, Lahore, Pakistan.

[8] Mechanical Engineering Department, College of Engineering, Taif University, P.O. Box 11099, Taif 21944, Saudi Arabia.

[9]Department of Mechanical Engineering, P. A. College of Engineering (Affiliated to Visvesvaraya Technological University, Belagavi), Mangaluru 574153, India.

Correspondence: ♣yewhengteoh@usm.my, †umitagbulut@duzce.edu.tr, asif.afzal86@gmail.com

Abstract

Fossil fuels are the primary source of energy for most industries worldwide. However, its resources are finite and declining day by day, and toxic gases are released due to their consumption which causes global warming and problems with the health of the living. Therefore, any alternatives to fossil fuels or any additives added to the fuel needed to be found to minimize fuel consumption and the emission of harmful gases. In this study, a spark-ignition engine fuelled with blends of petrol with different concentrations of graphite nanoparticles, Fe_2O_3 nanoparticles, and tire pyrolysis oil (TPO) were used to conduct energy, exergy, economic, and sustainability analyses, and the obtained results were compared with neat petrol. The blends of petrol with 40 mg/liter, 80 mg/liter, and 120 mg/liter of graphite nanoparticles & Fe_2O_3 nanoparticles, as well as 5% & 10% TPO, were used in a single-cylinder, four-stroke, air-cooled SI engine in this study. The experiments were conducted on various engine loads of 2 Nm to 10 Nm with an increment of 2 Nm at a constant speed of 3500 rpm. The maximum exergy and energy efficiencies were obtained 23.05% and 21.94% at a load of 8 Nm when the testengine fired with the P120FO blend, respectively. A maximum sustainability index of 1.3 for the P120FO blend was obtained. A minimum exhaust energy rate of 0.03241 kW was obtained for P120FO. A minimum exhaust exergy rate of 0.005849 kW was obtained for P90T10. Best results in energy efficiency, exergy efficiency, sustainability index, and economic analysis were obtained for the P120FO blend compared to neat petrol. Finally, it was concluded that the addition of nanoparticles in fossil fuel increases the engine's efficiency, decreases fuel consumption, and reduces the emission of harmful gases.

Keywords: Nano-fuel additives; Graphite; Ferric oxide; Tire pyrolysis oil; Exergy; Sustainability

1. Introduction

Petrol nowadays is one of the world's most widely used fossil fuels [1,2]. One of the leading industries that consume fuels and emit harmful emissions is the automotive industry [3]. Because petrol is a limited fossil type of energy and its costs continually change, research has been launched into alternate fuels that might be utilized in IC engines [4,5].

In the 1970s, the petrol-methanol mixture started to be replaced by petrol due to the oil shortage. Methanol is much easier to produce than petrol [6]. Just as methanol's octane index is larger than petrol, which is deemed an advantage, methanol-lethal heat is considered a drawback of this additive [7]. Several research studies have been conducted to add additives in base petrol [8,9]. Man et al. [10] reported that owing to its high octane number, alcohol in petrol has partially become trendy. Elfasakhany [11] studied the effects of mixtures of petrol-methanol, petrol-ethanol, and ethanol-petrol-methanol on the emission and performance parameters of the engine. It was examined that the mixture of methanol-ethanol-benzene showed the best effect on reducing the engine's exhaust emission and engine performance parameters. Al-Hassan [12] indicated that the exhaust emissions from engines were decreased. The engine's performance parameters were improved when the spark-ignition engine fired with the ethanol- petrol blend. It was mentioned in the study that the volumetric efficiency (VE), brake power (BP), and brake thermal efficiency (BTE) were increased by 8.3%, 9%, and 7%. Hsieh et al. [13] tested the spark-ignition engine by adding 10%, 20%, and 30% ethanol in fuel. It was concluded that fuel consumption (FC) and torque output of the engine was partially increased when it fired with the petrol-ethanol blend compared to when it fired with pure petrol. Yanju et al. [14] operated a 3-cylinder spark ignition engine fuelled with petrol blends with different percentages of methanol like 10%-35% with an increment of 5%. It was noted from the study that as the percentage of methanol increased in petrol, the value of brake power and torque decreased while the value of brake thermal efficiency (BTE) increased.

The possibility of obtaining fuels from scrap vehicle tires has become more appealing in recent years, especially when combined with a pyrolysis process since it has a huge potential to be used as

a fuel additive in internal combustion engines [15]. Furthermore, waste tires are used as a feedstock in the integrated gasification combined cycle (IGCC) for hydrogen, freshwater, and power production [16]. However, the diesel-TPO blends were found abundantly in the literature, while on petrol-TPO blends, no studies were found in the literature.

Few studies focused on petrol engines fired with a blend of fuel with nanoparticles like TiO_2, Mn_2O_3, and Fe_2O_3 to improve performance parameters and reduce petrol engine exhaust emissions [17]. Chan et al. [18] used the Di-Methyl Carbonate additive in petrol and mentioned reducing the emissions of unburnt hydrocarbons and particulate matter by 30% and 60%, respectively. Valihesari et al. [19] fired petrol engines by using nanoparticles like TiO_2, Fe_2O_3 proposed in the study an improvement in engine performance parameters and a reduction in exhaust emission of pollutant gases when fired with nanoparticles, as mentioned earlier as an additive in a petrol engine. Oh et al. [20] examined the effects of hydrogen nanobubble additive in petrol. It was mentioned in the study that brake-specific fuel consumption (BSFC) was improved from 291.10 g/kWh to 269.48 g/kWh, and power was enhanced by 4%. Amirabedi et al. [21] investigated the effects of Mn_2O_3 additive in petrol and proposed excessive oxygen bonds; decreased unburnt hydrocarbons and CO; increased CO_2 and NOx. The study also mentioned that the blend of 20 ppm Mn_2O_3- petrol-10% ethanol was best in terms of lowering unburnt hydrocarbons (UH) and brake specific fuel consumption (BSFC). Ali et al. [22] reviewed the effects of the blends of TiO_2/Al_2O_3 with petrol on fuel consumption (FC) and economy. It was noted from the study that in the new European driving cycle, 4 L/100 km was saving in fuel consumption. Taghavifar et al. [23] used newly generated nanomaterial TNA (TiO_2) to make a blend with pure petrol and with bioethanol- petrol. The four blends samples were used, namely pure petrol, 20% bioethanol-80% petrol, 100 ppm TNA-pure petrol, and 20% bioethanol-100 ppm TNA- 80% petrol. Adding TNA as an additive during the combustion process showed a better oxidation process. The study also listed that the engine's heat exchange increased, and exhaust emissions decreased. Analyses of energy and exergy may be conducted by utilizing the performance parameters received from the IC engines' tests [24].

In recent years, many studies have been conducting for exergy analysis by using alcoholic or alternative fuel [25]. Alasfour [26] carried out an experimental analysis on exergy using a single-cylinder, spark-ignition engine fired with a blend of petrol-butanol. It was reported in the study that 50.6% of fuel energy could be used for practical work, and the unaccounted-for usable energy comprises 49.4% of the accessible total energy. Compared to pure petrol, the 2nd law thermodynamic efficiency for petrol-butanol blend decreased by 7%, reflecting that it was inappropriate and undesirable. Sezer and Bilgin [27] fired the petrol engine with a petrol-ethanol blend; by defining the distribution of energy and energy lost by cooling, exhaust, and radiation, it is possible to determine the optimum working interval. Since the irreversible processes increase the engine's energy loss, it decreases the exergy. Ghazikhani et al. [25] used a two-stroke engine fired with a petrol-ethanol blend to check its effects on exergy analysis. The internal combustion irreversibility increased when the IC engine was run using alcoholic fuel. This is because of the increase in temperature difference between the unburned mixture and burned combustion products, which happened because of the alcohol additive's rapid evaporation. Different outcomes were obtained when a low percentage of ethanol (5%) was used as an additive, and using alcohol as an additive was very beneficial and desirable for this condition via the second law viewpoint. The study also noted that emissions of CO_2, CO, HC, and NOx had been significantly decreased in all conditions. Mithaiwal et al. [28] conducted an engine performance test focused on exergy analysis by using blends of 75% petrol – 25% ethanol, 60% petrol – 40% ethanol, and 100% ethanol. Mechanical efficiency reduced by 3-5% when engine operated with 100% ethanol, 10-16% decreased when blend consists of 25% ethanol, 5-9% decreased when blend consists of 40% ethanol as compared to when engine fuelled with 100% petrol. Ozcan and Cakmak [29] studied the effects of the blend of petrol with oxygenated fuel additive involving 10% methanol, 10% ethanol, and 10% solketal on the exergy parameters in a spark-ignition engine. As compared to petrol, exergy efficiencies decreased, and the maximum pressures of the cylinder increased when the engine fired with an oxygenated fuel additive. It was mentioned that the maximum decrease in exergy efficiency was 8.42% when the blend consisted of 10% solketal. It was also noted

that minimum irreversibility has appeared with fuel having 10% ethanol while maximum irreversibility has occurred with pure petrol fuel. Additionally, first law efficiency decreased with these oxygenated additives.

A sustainability analysis determines a system's capacity to sustain itself. The goal of sustainability is to meet current demands while also considering future concerns [30]. Dogan et al. [31] determine the exergy efficiency-based sustainability index. Alternative to pure petrol, the blend of 10% ethanol- 90% petrol and 10% methanol- 90% petrol are also used. It was mentioned in the study that the sustainability index's value could be increased by decreasing the thermodynamic irreversibility that took place in combustion processes. It was also noted that the sustainability index value also increased as energy and exergy efficiencies increased by increasing the engine load. The maximum value of sustainability at 100% load was 1.26 when the engine fired with pure petrol.

The detailed literature review of spark ignition engines fuelled with petrol-nanoparticles blends is presented in **Table 1.** Literature review revealed that the impact of Fe_2O_3-petrol and graphite-petrol blends on the engine's performance had been studied in terms of BSFC, engine torque, BTE, engine power, and exhaust emissions. However, while exergy analysis is a valuable tool for determining the efficiency of a thermal system, it has not been used to evaluate the performance of spark ignition engines that operate on Fe_2O_3-petrol and graphite-petrol blends. For the first time, energy, exergy, economic, and sustainability assessments were carried out on a single-cylinder, air-cooled, four-stroke, spark-ignition engine fuelled with Fe_2O_3-petrol and graphite-petrol blends with different volumetric fractions under various engine loads and constant crankshaft speed conditions. The Tire Pyrolysis Oil as a fossil fuel alternative in a spark-ignition engine is used to encourage this first step. Since no studies using TPO-petrol blends have been found in the literature, this research is the first to involve blending TPO with petrol fuel. The energy, exergy, economic, and sustainability analyses for Fe_2O_3-petrol, graphite-petrol, and TPO-petrol blends were evaluated compared to neat petrol. The aim of the research is the Global SDGs (Sustainable Development Goals), which improve motivation by all countries.

Table 1: Literature Review.

Type of engine	Parent fuel	Blend	Performance Parameters	Emission Parameters	References
Four-stroke, 1 cylinder, SI engine	Petrol	Methanol-ethanol-benzene	BP▲ η_v▲ T▲	CO▼ UHC ▼ CO_2▲	[11]
Four strokes, 4-cylinder, SI engine	Unleaded petrol	Ethanol-blend	η_v▲ BP▲ BTE▲ BSFC▼	Exhaust Emissions▼	[12]
1600 cm^3 multi-point injection spark ignition engine	Petrol	Ethanol	FC ▲ T ▲	CO ▼ HC▼ CO_2▲	[13]
3-cylinder, 4-stroke, port fuel injection, Spark-ignition engine	Petrol	Methanol	BP ▼ T▼ BTE ▲	CO ▼ NOx ▼ CH_3OH▲	[14]
petrol engine	Petrol	TiO_2, Mn_2O_3, Fe_2O_3	Performance Parameters ▲	Exhaust emissions ▼	[17]
Four-cylinder turbocharged, direct-injected petrol engine	Petrol	Di-Methyl Carbonate additive in petrol	---	UHC▼ PM ▼	[18]
4-cylinders, 4-stroke petrol engine	Petrol	TiO_2, Fe_2O_3	BP▲ T▲	Exhaust emission ▼	[19]
4-cylinder, port fuel injection petrol - fuelled SI engine	Petrol	Hydrogen nanobubble	BSFC▲ BP▲	---	[20]
EF7 four-cylinder, four-stroke, water-cooled, SI engine	Petrol	Ethanol + Mn_2O_3	BP▲	HC▼ CO▲ CO_2▲ NO_x ▲	[21]
4-cylinder, 4-stroke, naturally aspirated, petrol engine	Petrol	TiO_2/Al_2O_3	BP ▲ T▲ η_m▲ BSFC▼	---	[22]
4-cylinder, 4-stroke, water-cooled, spark-ignition	Petrol	Bioethanol-petrol, TNA	BSFC ▼	CO ▼ HC ▼ CO_2▼ NO_x ▼	[23]
Two-stroke, spark-ignition engine	Petrol	Petrol - ethanol	---	CO ▼ HC ▼ CO_2▼ NO_x ▼	[25]
Single-cylinder, water-cooled, four-stroke engine	Petrol	Methanol 10%, ethanol, and 10% solketal	ψ ▼ P (cylinder) ▲	---	[29]

Spark-ignition (SI) engines	Petrol	Ethanol and methanol	Entropy ▼ W_{out} ▼ FC ▲ BSFC ▲	Exhaust emission ▼	[32]
4-stroke, Single cylinder, water-cooled (SI) engine	Petrol	Ethanol & methanol	ψ ▲ η ▲	CO ▼ HC ▼ CO_2 ▼ NO_x ▼	[31]

2. Experimental Methods

2.1. Tested Fuel

Iron oxide (Fe_2O_3) & graphite (G) nano-additives were procured from a local company and used as received. Iron oxide, which contains 99 percent Fe_2O_3 and is used as a combustion catalyst in IC engines, and graphite powder, which contains 90 percent carbon and is used as a lubricant in IC engines. The nomenclature of the tested fuels is listed in **Table 2.**

Table 2: Nomenclature of fuel and design of Experiment.

Exp.	**Additives**	**Concentrations**	**Fuel Nomenclature**	**Test scheme**
1.	Neat Petrol	-	P	Each test is performed at the engine torque of 2 to 10 Nm with an increment of 2 Nm with a constant speed of 3500 rpm.
2.	Iron Oxide (Fe_2O_3)	40 mg/l	P40FO	
3.		80 mg/l	P80FO	
4.		120 mg/l	P120FO	
5.	Graphite	40 mg/l	P40G	
6.		80 mg/l	P80G	
7.		120 mg/l	P120G	
8.	TPO	5%	P95T5	
9.		10%	P90T10	

There is no narcotic, poisonous, or unpleasant nanoparticles' characteristics to cause extreme human irritation or discomfort. These nanoparticles have excellent properties, including high thermal conductivity [33], high surface-to-volume ratios [34], strong electrical conductivity, and unusual combustion-catalytic activities [34].

At the beginning of the waste tire pyrolysis oil (TPO) extraction procedure, the rubber and steel wires from the scrap tires must be isolated and discarded, with only a shredded tire being used

to cut the tire into small sections. The waste tire pieces reacted in a thermal chamber during the pyrolysis process. The reaction temperature in the pyrolysis chamber rises from 400 to 600 °C during fluid tire pyrolysis oil production. The current research obtained waste TPO from the Pakistan pyrolysis industrial setup.

2.2. Fuel Preparation

The reference fuel, commercial petrol, was purchased from the local station of PSO (Pakistan State Oil).

Table *3* displays the physical and chemical properties of neat petrol. 40 mg/liter, 80 mg/liter, and 120 mg/liter concentrations of graphite nanoparticles & iron oxide (Fe_2O_3) nanoparticles, and 5% & 10% TPO were added to clean petrol and stirred continuously for thirty minutes in the 79-1 hot plate magnetic stirrer to make well-homogenized blends of the fuel. These fuel blends were poured directly into the fuel tank supplied upstream of the petrol engine test bed's fuel flow measuring burettes.

The graphite and Fe_2O_3 nanoparticles addition have no noticeable effect on the physicochemical properties of the fuel blends compared to the reference fuel or neat petrol (as illustrated in

Table *3*), so the use of these blended fuels is a standard petrol engine can be justified without any changes. A 0.16% density increase, a reduction of 3.6% in kinematic viscosity, and a 0.06% rise in the calorific value were observed for FO blends. The G blends have seen a maximum reduction of 3.7% in kinematic viscosity, a 0.2% rise in density, and a 0.04% improvement in the calorific value.

On the other hand, there is a remarkable change in the kinematic viscosity of fuel blends in the case of TPO as compared to the neat petrol, as illustrated in

Table *3*. There is a maximum increase of 14.54% in kinematic viscosity. However, the TPO addition has no noticeable effect on the density and calorific value of the blended fuels compared to

neat petrol. The maximum rise of 1.778% in density and a reduction of 0.308% in calorific value was observed for TPO blends.

Table 3: The key physical and chemical properties of the fuels.

	Density @15 ºC (kg/m^3) ASTM D1298	**Kinematic viscosity @40 ºC (cSt) ASTM D445**	**Clorific value (MJ/kg) ASTM D240**
P	748	0.55	44.11
P40FO	749.2	0.53	44.13
P80FO	750.1	0.52	44.17
P120FO	751.3	0.51	44.19
P40G	749.5	0.54	44.12
P80G	750.4	0.52	44.13
P120G	751.9	0.5	44.15
P95T5	753.7	0.58	43.97
P90T10	761.3	0.63	43.83

2.3. Testengine and Operating Conditions

As shown in **Figure 1**, the apparatus used for this analysis was arranged and set up. A single-cylinder, 4-stroke, air-cooled, spark injection engine was the testengine. The features of the testengine and dynamometer are given in **Table 4** and **Table 5,** respectively. The engine operates at a maximum torque of 11.3 Nm and a maximum power of 4.2 kW. In the unmodified testengine that always runs at 3500 rpm and variable load, each fuel test was performed under ambient temperature 25 ºC. Torque & brake power were measured at 3500 rpm of the testengine, using an eddy current dynamometer. In the meantime, a gas analyzer was used to assess the emission level of several gas exhausts directed from the engine to the gas analyzer.

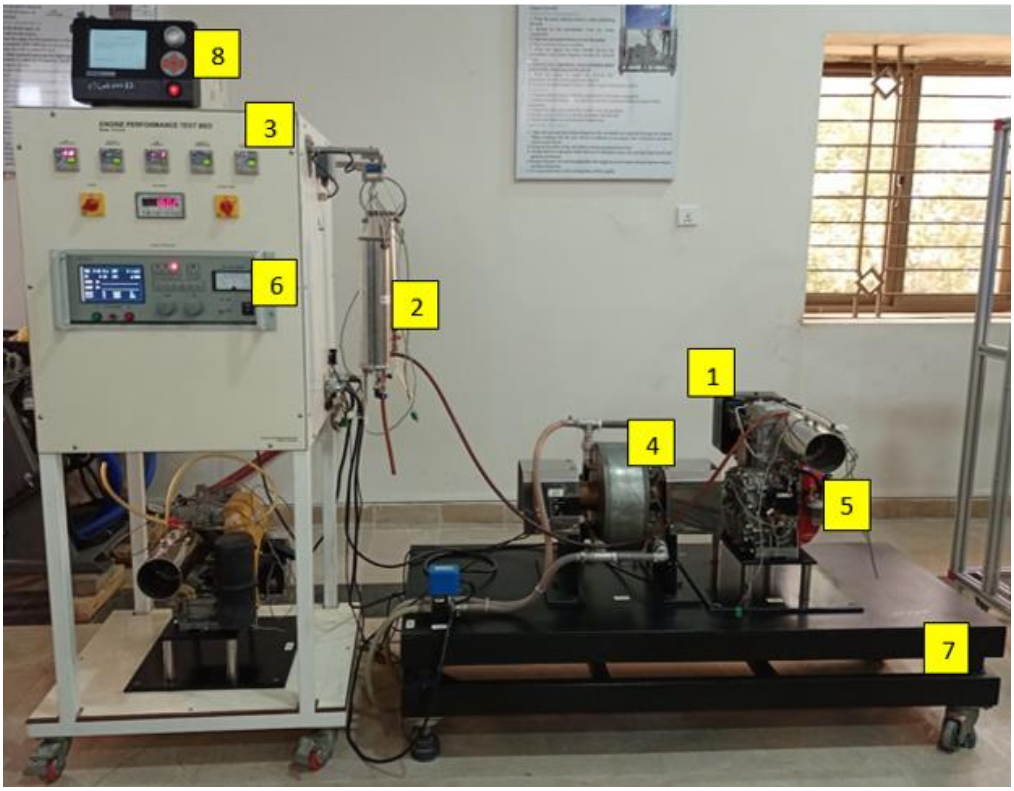

Figure 1: Experimental setup.

1	Exhaust pipe	2	Fuel tank
3	Control panel	4	Dynamometer
5	Petrol engine	6	Dynamo controller
7	The base of the engine testbed	8	Exhaust gas analyzer

Table 4: The engine parameters.

Type	4-stroke single-cylinder petrol (spark ignition) engine
Model	EY28D
Brand	Robin Engines
Bore x stroke	75 x 62 mm
Piston displacement	273 cc (cm^3)
Maximum output	4.2 kW / 4000 rpm
Maximum torque	11.3 Nm / 2500 rpm
Spark plug	NGK BR-6HS
Lubricant	Automotive lubricating oil (API/SE or advanced grade, SAE/10W-30)
Starting system	Recoil starter
Ignition system	Flywheel magneto type
Cooling system	Forced air cooling

Carburetor	Horizontal draft, float type

Table 5: Eddy current dynamometer specifications in the engine testbed.

Brand	Xiang Yi
Model	GW 10
Rate absorbing power	10 kW
Rated maximum speed	13000 RPM
Measuring the accuracy of rotational speed	± 1 r/min
Rated braking torque	50 Nm
Measuring the accuracy of torque	± 0.2-0.3% FS
Coolant	Freshwater

2.4. Uncertainty analysis

The following equation, which gives the total uncertainty value for this model, is used to perform the uncertainty analysis [35].

$$W_R = [(\frac{\partial R}{\partial x_1} w_1)^2 + (\frac{\partial R}{\partial x_2} w_2)^2 + ...(\frac{\partial R}{\partial x_n} w_n)^2]^{\frac{1}{2}} \quad (1)$$

Here, w indicates the dimension of shape factor, W_R (%) shows system uncertainty, R indicates total function uncertainty, and n is the total number of independent variables used in the study. Accuracy specifications of measuring instruments are given in **Table 6**.

The overall uncertainty for this study was found to be 1.74% based on this calculation. This is within the permissible range.

Table 6: Accuracy specifications of measuring instruments.

Measurement type	**Range**	**Accuracy**	**Techniques**	**% Uncertainty**
Load	±50 Nm	±0.1 Nm	Strain gauge type load cell	±0.25
Engine Speed	0-13,000 rpm	±1 rpm	Magnetic pick-up type	±0.1
Fuel flow	0.5-36 L/hr	±0.04 L/hr	Positive displacement gear wheel flow meter	±0.5
Air flow	0.25-7.83 kg/min	±0.07 kg/min	Hot wire air mass meter	±2
CO emission	0-10% volume	±0.001%	Non-dispersive infrared	±1

CO_2 emission	0-10% volume	±0.001%	Non-dispersive infrared	±1
NO_x emission	0-5,000 ppm	±1 ppm	Electrochemical	±1.3
Pressure	0-25,000 kPa	±10 kPa	Piezoelectric crystal type	±0.5
Temperature	0-1200°C	±0.3°C	Thermocouple (Type K)	±0.15
Calculated				
$E\dot{n}_{air}$		±0.004688 kW		±0.3
$E\dot{n}_{fuel}$		±0 kW		±0
$E\dot{n}_{w}$		±0.008342 kW		±0.26
$E\dot{n}_{exh}$		±0.0007613 kW		±0.34
$E\dot{n}_{loss}$		±0.009287 kW		±0.07
η_{en}		±0.05153%		±0.27
$E\dot{x}_{air}$		±0.00001348 kW		±0.89
$E\dot{x}_{fuel}$		±0 kW		±0
$E\dot{x}_{w}$		±0.008342 kW		±0.26
$E\dot{x}_{exh}$		±0.0002478 kW		±0.39
$E\dot{x}_{loss}$		±0.001205 kW		±0.07
$E\dot{x}_{dest}$		±0.007294 kW		±0.06
ψ_{ex}		±0.05321%		±0.26
R_{en}		±0.0000004644 (kW/$)		±0.07
$R_{ex,loss}$		±0.00000006024 (kW/$)		±0.07
$R_{ex,dest}$		±0.0000003647(kW/$)		±0.06

3. Theoretical procedure

This study analyzes the energy, exergy, economics, and sustainability analysis of blends of ferric oxide and graphite with petrol with different blending ratios. In **Table 7**, the experimental data is given.

The following assumptions were assumed when performing the analyses, as mentioned earlier.

- The experimental setup (engine) is operated in a steady-state condition with a steady flow.
- The exhaust gases are ideal gases exposed to the environment, and the supplied air to the engine is also ideal.

- The change of potential energy and exergy, kinetic energy, and exergy of the system is negligible.
- The dead state temperature (T_o) and pressure (P_o) are 298.16 K and 101 kPa, respectively.

Table 7: The experimental data.

Fuel	Load (Nm)	$\dot{m}_{fuel}$ (kg/h)	$\dot{m}_{air}$ (kg/h)	CO (vol.%)	CO_2 (vol.%)	HC (ppm)	O_2 (vol.%)	NO (ppm)	T_{air} (^oC)	T_{exh} (^oC)	T_{engine} (^oC)
P	2	0.84	10.69	0.13	3.19	6	17	26	35.5	157	60
	4	0.84	12.42	0.22	15.34	6	15.45	105	37	195.9	62
	6	1.2	14.43	0.27	13.21	11	13.73	290	38.3	214.8	65.2
	8	1.32	17.71	0.36	7.71	19	10.74	728	39	237.4	68.5
	10	1.32	20.43	0.14	9.38	12	8.52	1134	39.7	269.2	69.4
P40FO	2	0.72	10.39	0.15	3.1	16	16.79	20	36.4	175.6	60.10
	4	0.9	12.49	0.17	4.33	10	15.24	98	37.9	207.3	62.01
	6	0.96	15.11	0.14	5.77	10	13.2	299	38.2	226.9	65.40
	8	1.38	17.89	0.19	7.54	10	10.76	681	39.2	248.1	69.00
	10	1.38	20.67	0.42	9.65	16	7.75	1175	39.6	275.2	70.30
P80FO	2	0.78	10	0.19	2.77	0	17.42	0	36.7	152.8	60.15
	4	0.72	11.67	0.29	3.52	0	16.04	56	37.6	179.9	62.52
	6	0.96	14.31	0.27	5.23	0	13.83	242	38.7	211.2	65.50
	8	1.32	17.39	0.38	7.39	0	10.85	638	39.6	242.3	69.02
	10	1.5	20	0.19	9.17	0	8.2	1121	40.3	264.9	70.43
P120FO	2	0.66	7.291	0.37	3.77	270	3.78	41	40.6	206.5	60.10
	4	0.6	8.83	0.19	4.67	109	14.23	165	40.2	196.7	62.58
	6	0.66	10.14	0.06	5.42	30	13.55	315	40.3	200.5	65.52
	8	0.72	12.02	0.04	6.45	26	12.29	640	40.5	212.4	69.03
	10	0.9	13.4	0.04	7.1	27	11.2	1114	40.5	230.1	70.56

P40G	2	0.66	9.287	0.39	3.22	32	16.24	52	41.6	218.5	60.00
	4	1.32	10.41	0.48	3.22	13	15.68	88	41.3	206.1	62.04
	6	1.14	13.96	0.84	4.97	30	13.55	246	41.6	216.2	65.45
	8	1.32	17.22	0.93	6.65	39	11.08	539	42.4	238.4	68.7
	10	1.56	20.37	0.81	8.68	43	8.4	1170	42.8	263.3	70.5
P80G	2	0.78	10.46	0.12	3.5	6	15.97	34	41.2	224.4	60.07
	4	0.96	12.75	0.12	4.55	0	14.76	98	41.8	224.5	62.5
	6	1.2	15.24	0.08	5.93	0	13.05	293	41.6	234.8	65.60
	8	1.26	18.53	0.11	7.67	0	10.42	656	41.5	253.9	68.90
	10	1.38	19.29	0.24	9.59	6	7.98	967	42.3	284.5	71.02
P120G	2	1.02	10.69	0.07	3.05	34	16.86	20	35.9	176.2	60.30
	4	0.96	13.12	0.12	4.66	30	14.77	114	37	206.4	62.76
	6	1.14	14.97	0.12	6.04	27	12.92	353	38	232.1	65.70
	8	1.2	17.98	0.20	7.92	30	10.21	703	38.6	250.8	69.42
	10	1.5	20.46	0.22	9.82	28	7.78	1145	38.9	274.2	70.05
P95T5	2	0.78	9.64	0.002	0.05	27	20.89	0	31.4	104.5	58.52
	4	0.72	11.57	0.22	5.50	41	13.44	246	33.4	175.2	60.23
	6	0.96	14.56	0.16	6.58	40	12.65	515	33.7	210.1	62.50
	8	1.08	17.62	0.09	8.50	31	9.85	500	33.9	237.4	65.34
	10	1.2	20.81	0.13	8.51	35	9.59	1226	34.7	273.1	67.21
P90T10	2	0.84	9.661	0.11	2.44	78	17.80	35	31.3	84.7	58.02
	4	0.84	14.43	0.20	3.36	66	16.49	122	32.8	159.3	61.33
	6	1.02	14.38	0.08	4.71	56	14.82	347	33.7	206.3	63.15
	8	1.32	16.93	0.14	6.38	55	12.60	779	34.8	231.7	65.42
	10	1.26	19.97	0.17	7.98	55	10.48	1148	35.9	255.1	69.01

3.1. Energy analysis

When the system is in a steady-state, the energy balance is carried out by the law of conservation of energy and energy balance and can be written as:

$$\sum E\dot{n}_{in} = \sum E\dot{n}_{out} \tag{2}$$

Equation (2) can also be written as:

$$E\dot{n}_{air} + E\dot{n}_{fuel} = E\dot{n}_{w} + E\dot{n}_{exh} + E\dot{n}_{loss} \tag{3}$$

Here, $E\dot{n}_{air}$ shows the energy rate of the supplied air to the testengine, $E\dot{n}_{fuel}$ shows the energy fuel rate supplied to the testengine, $E\dot{n}_{w}$ shows the energy rate of the produced work by the testengine, $E\dot{n}_{exh}$ shows the energy rate of gases exhausted by the testbed of the engine, and directed towards the atmosphere, and $E\dot{n}_{loss}$ represents the rate of energy loss due to the heat transfer of the engine and directed towards the environment.

$E\dot{n}_{air}$ shows in equation (3) could be calculated as:

$$E\dot{n}_{air} = \dot{m}_{air} h_{air} = \rho_{air} \dot{V}_{air} h_{air} \tag{4}$$

Where; ρ, h, $\dot{m}$ and $\dot{V}$ are representing the specific density, enthalpy, mass flow rate, and volume flow rate of air, respectively.

$E\dot{n}_{fuel}$ shows in equation (3) could be calculated as:

$$E\dot{n}_{fuel} = \dot{m}_{fuel} H_u \tag{5}$$

Here, H_u represents the lower heating value of fuel or calorific value of the fuel.

$E\dot{n}_{w}$ shows in equation (3) could be calculated by the following equation:

$$E\dot{n}_{w} = \omega T \tag{6}$$

Where ω and T are the angular velocity and torque of the testengine respectively & angular velocity of testengine can be originated as:

$$\omega = \frac{2\pi n}{60} \tag{7}$$

Where n shows the angular speed of the crankshaft.

$E\dot{n}_{exh}$ can be found by the following equation:

$$E\dot{n}_{exh} = \sum_{i=1}^{n} \dot{m}_i h_i = \dot{m}_{CO} h_{CO} + \dot{m}_{NO_x} h_{NO_x} + \dot{m}_{CO_2} h_{CO_2} + ... \tag{8}$$

h_i , $\dot{m}_i$ represent the specific enthalpy of exhaust gases and mass flow rate, respectively.

After finding all the terms involving in equation (3), the $E\dot{n}_{loss}$ can easily be calculated by this energy balance equation:

$$\eta_{en} = \frac{E\dot{n}_w}{E\dot{n}_{air} + E\dot{n}_{fuel}} \tag{9}$$

3.2. Exergy analysis

The utilization of total energy cannot be done by only considering energy analysis. It does not provide an idea about the usefulness and quality of all energy sources that can egress in product and waste and cross the confines [36]. For more accurate results, exergy analysis is to be used.

Exergy is a non-conserved quantity and can be destroyed. Consequently, the steady-state exergy balance system will establish a new expression, exergy destruction. Exergy balance for the steady-state system is:

$$\sum E\dot{x}_{in} = \sum E\dot{x}_{out} + \sum E\dot{x}_{dest} \tag{10}$$

The equation of exergy balance is given below:

$$E\dot{x}_{air} + E\dot{x}_{fuel} = E\dot{x}_w + E\dot{x}_{exh} + E\dot{x}_{loss} + E\dot{x}_{dest} \tag{11}$$

Where $E\dot{x}_{air}$ shows the exergy rates of air supplied, $E\dot{x}_{fuel}$ shows the exergy rates of fuel supplied, $E\dot{x}_{exh}$ shows the exergy rates of exhaust gases discharged into the atmosphere, $E\dot{x}_w$ shows the work

generated by the testengine, $E\dot{x}_{dest}$ shows the exergy destruction rate, and $E\dot{x}_{loss}$ exergy loss rate. $E\dot{x}_{air}$ exergy rates of air supplied could be calculated by using the given equation:

$$E\dot{x}_{air} = \dot{m}_{air} C_{p,air} [(T_{air} - T_0) - T_0 \ln(\frac{T_{air}}{T_0})] \quad (12)$$

Where T represents the temperature and C_p represents the specific heat capacity. $E\dot{x}_{fuel}$ (fuel supplied exergy rate for the testengine) is given below:

$$E\dot{x}_{fuel} = \dot{m}_{fuel} H_u \varepsilon_{fuel} \quad (13)$$

Where ε_{fuel} is the chemical exergy factor and it can be found by given [37];

$$\varepsilon_{fuel} = 1.0401 + 0.1728\frac{H}{C} + 0.0432\frac{O}{C} + 0.2169\frac{\alpha}{C}[1 - 2.0628\frac{H}{C}] \quad (14)$$

Where α represents the Sulphur of fuel, C represents the mass ratios of carbon, H represents the Hydrogen, O represents the Oxygen, and the mass fractions of given elements are (C, H, O, N and α) listed in **Table 8** determined via ultimate analysis.

Table 8: The mass fraction of carbon, hydrogen, oxygen, and sulfur of tested fuels.

	C	**H**	**O**	**N**	**α**
P	87.4	12.6	0	0	0
P40FO	78.3	12.5	0.2	0	0
P80FO	87.1	12.4	0.5	0	0
P120FO	86.9	12.3	0.8	0	0
P40G	87.4	12.6	0	0	0
P80G	87.4	12.6	0	0	0
P120G	87.4	12.6	0	0	0
P95T5	87.38	12.58	0.03	0	0.005
P90T10	87.39	12.59	0.01	0	0.01
TPO	87.15	9.63	1.57	0	1.65

The energy and exergy rate of work is equal. So, $E\dot{x}_w$ the exergy rate generated by work is calculated by the given equation:

$$E\dot{x}_w = E\dot{n}_w = \omega T \tag{15}$$

Exhaust gases exergy rate $E\dot{x}_{exh}$ released to the environment can be calculated by the given equation:

$$E\dot{x}_{exh} = \sum_{i=1}^{n} \dot{m}_i (ex_{tm,i} + ex_{ch,i}) \tag{16}$$

Here, $ex_{tm,i}$ and $ex_{ch,i}$ are the specific physical and specific chemical exergy rates for the exhaust gases. For i_{th} compound the $ex_{tm,i}$ and $ex_{ch,i}$ can be calculated by using the following equations, respectively:

$$ex_{tm,i} = C_{p,i}[(T_{exh} - T_0) - T_0 \ln(\frac{T_{exh}}{T_0})] \tag{17}$$

$$ex_{ch,i} = \bar{R} T_0 \ln(\frac{y_i}{y_{env,i}}) \tag{18}$$

Where the exhaust gas temperature and Universal gas constant are represented by T_{exh} & $\bar{R}$, T_0 represents the ambient temperature, $y_{env,i}$ and y_i represent i_{th} compound molar fraction for the environment and exhaust gases, respectively. **Table 9** represents the values of the molar fractions of exhaust gases for the environment ($y_{env,i}$).

Table 9: Composition (molar fraction) of exhaust gases for the atmospheric air [38].

Elements	**Molar Fractions (%)**
N_2	75.6700
CO	0.00070

CO_2	0.03450
H_2O	3.03000
H_2	0.00005
SO_2	0.00020
O_2	20.3500
Others	0.91455

The exergy rate of loss energy rate can be calculated for the testengine is given below:

$$E\dot{x}_{loss} = E\dot{n}_{loss}(1-\frac{T_0}{T_{engine}}) \tag{19}$$

T_{engine} represents the testengine block temperature. The exergy destruction rate can be calculated by solving all the terms involved in equation (11).

The testbed engines efficiency for exergy can be found by using this equation:

$$\psi = \frac{E\dot{x}_w}{E\dot{x}_{air} + E\dot{x}_{fuel}} \tag{20}$$

3.3. Thermoeconomic analysis

Thermo-economic shows the combination of economics and thermodynamics. For the thermo-economic analysis, the Exergy Cost Energy Mass Method (EXCEM) was found in literature and 1st introduced by Rosen and Dincer [39] in 2003. By using the EXCEM method, the equation of cost balance for thermo-economic analysis can be calculated as:

$$K_{in} = K_{gen} - K_{out} = \Delta K \tag{21}$$

Here, K_{gen} shows the generation cost, and this term consists of the capital cost like cost on maintenance and operation expenditures. The cost generation equation is given:

$$K_{gen} = K_{cap} - K_{O-M} - K_{OCC} \tag{22}$$

K_{OCC}, K_{O-M} and K_{cap} represent other capital costs, operational & maintenance costs, and capital costs, respectively. The main objective of the thermos-economic analysis is to provide the information and relation between the energy loss and capital cost. The thermos-economic parameter equation is given [40].

$$R_{en} = \frac{E\dot{n}_{loss}}{K_{cap}} \tag{23}$$

R_{en} shows the thermoeconomic parameter that gives the information of total energy loss over capital investment cost. Moreover, the relation of exergy destruction and exergy loss with capital investment cost can be calculated by using the given equation [36].

$$R_{ex,loss} = \frac{E\dot{x}_{loss}}{K_{cap}} \tag{24}$$

$$R_{ex,dest} = \frac{E\dot{x}_{dest}}{K_{cap}} \tag{25}$$

$R_{ex,dest}$ and $R_{ex,loss}$ are the significant values that denoted the value of exergy destruction per capital investment cost and the exergy loss per capital investment cost, respectively.

3.4. Sustainability analysis

Sustainability priorities to meet current needs without reducing the opportunity to meet the demands of future ages. Sustainability depends on environmental protection, social expansion, and economic development. The growth of sustainability can be achieved with the efficient use of energy assets. Exergy efficiency and energetic efficiency of systems are significant factors due to sustainable development. Some of the parameters were applied in this experiment to determine the sustainability of the process. Moreover, the improvement potential (IP) is also included in this method. If the irreversibility of the process is reduced and it can be very well measured, the exergy IP of any process can represent the IP and can be determined by the following equation [41].

$$I\dot{P} = (1-\psi)(E\dot{x}_{in} - E\dot{x}_{out}) \tag{26}$$

Another sustainability parameter is the depletion number (DN). The depletion number equation plays a significant role in determining the efficiency of fossil fuel consumption (FFCE) [42]. It is written below:

$$DN = \frac{E\dot{x}_{dest}}{Ex_{in}} = (1-\psi) \tag{27}$$

Sustainability index (SI) is another significant parameter is sustainability index (SI) is the reciprocal of depletion number (DN) [40], which is written below:

$$SI = \frac{1}{DN} \tag{28}$$

4. Results and discussion

This study aimed to see how various Fe_2O_3, Graphite nanoparticles', and TPO's concentrations impacted energy, exergy, sustainability, and economic parameters in a 1-cylinder, 4-stroke, air-cooled, spark-ignition engine. Assessments of energy, exergy, sustainability, and economics were carried out for a load range of 2 to 10 Nm with an interval of 2 Nm, at a constant crankshaft speed of 3500 rpm. The results from the blended fuels (P40FO, P80FO, P120FO, P40G, P80G, P120G, P95T5, and P90T10) were compared to the results from neat petrol (P).

4.1. Energy analysis

Table 10 depicts the energy analysis results for the blended fuels studied in this study. As the load on the testengine increases, the energy rates of all the blended fuels fed to the testengine increase. For example, in the case of the P40FO blend, fuel energy rates at 2, 4, 6, 8, and 10 Nm are 8.82, 11.03, 11.77, 16.92, and 16.92 kW. Compared to other blends, petrol fuel had the highest fuel energy rate in each engine load except for some graphite blends (G). For example, at a 6 Nm engine load, the fuel energy rate of P is 14.7 kW, while the fuel energy rates of P40FO, P80FO, P120FO, P40G, P80G, P120G, P95T5, and P90T10 are 11.77, 11.78, 8.10, 13.97, 14.71, 13.98, 11.73, and 12.42 kW

respectively. Because of their high thermal conductivity [43], the graphite nanoparticles act as heat sinks for the nearby fuel droplets within the combustion chamber, increasing the fuel vaporization rate. As a result, nanoparticles are carried away from the fuel droplets after the fuel is converted to vapors, allowing for faster combustible combinations. When graphite nanoparticles are mixed with petrol, they enhance the combustion process inside the cylinder, resulting in a rise in fuel energy.

The rate of energy loss in the testengine for all the fuel blends increased as the engine load increased, like the rate of fuel energy. Except for some graphite blends, the testengine's energy loss rate was highest for neat petrol (P) at a given testengine load (G). For example, the testengine's energy loss rates were 8.84, 9.56, 8.13, 8.00, 9.56, 12.54, 9.75 and 10.47 kW for P40FO, P80FO, P120FO, P40G, P80G, P120G, P95T5 and P90T10 respectively, at a load of 2 Nm. For petrol, however, this value is calculated to be 10.33 kW.

The testengine's energy efficiency varies with the testengine load for the fuels considered in this study, as illustrated in **Figure 2**. The testengine's energy efficiency improved as the testengine load increased for each fuel taken into consideration. The P120FO had the highest energy efficiency of the testengine. This is because the fuel and air consumption need to produce the same amount of crankshaft work are lower than for other fuel blends. **Figure 2** also illustrated that FO blends had greater efficiencies than other blends at all the loads.

The rise in efficiency due to Fe_2O_3 nanoparticles is credited to additional oxygen (O_2) present in Fe_2O_3. Iron oxide (Fe_2O_3) undergoes a reaction with oxygen (O_2), present in the inlet air, and it produced extremely active species that help in the complete fuel combustion [44]. The presence of excess oxygen (O_2) in Fe_2O_3 allows the burning of more fuel molecules, resulting in greater energy efficiency. The maximum energy efficiency was found for P120FO is 21.94% at a load engine of 8 Nm in this analysis.

Table 10: The energy analysis results for the testengine fuelled with the considered fuels.

	P					**P40FO**				
Load (Nm)	2	4	6	8	10	2	4	6	8	10
	Energy analysis					Energy analysis				
$E\dot{n}_{air}$ (kW)	0.91	1.072	1.25	1.53	1.778	0.89	1.081	1.30	1.55	1.799
$E\dot{n}_{fuel}$ (kW)	10.29	10.29	14.7	16.17	16.17	8.82	11.03	11.77	16.92	16.92
$E\dot{n}_{w}$ (kW)	0.79	1.58	2.35	3.11	3.86	0.79	1.57	2.35	3.11	3.591
$E\dot{n}_{exh}$ (kW)	0.08	0.18	0.21	0.21	0.2775	0.08	0.12	0.16	0.22	0.29
$E\dot{n}_{loss}$ (kW)	10.33	9.59	13.38	14.37	13.38	8.84	10.41	10.56	15.14	14.83
η (%)	7.08	13.92	14.79	17.61	21.53	8.16	13.02	18.01	16.84	19.18
	P80FO					**P120FO**				
Load (Nm)	2	4	6	8	10	2	4	6	8	10
	Energy analysis					Energy analysis				
$E\dot{n}_{air}$ (kW)	0.86	1.00	1.24	1.513	1.744	0.63	0.76	0.88	1.049	1.169
$E\dot{n}_{fuel}$ (kW)	9.57	8.83	11.78	16.2	18.41	8.10	7.36	8.10	8.838	11.05
$E\dot{n}_{w}$ (kW)	0.79	1.58	2.35	3.116	3.733	0.57	1.09	1.63	2.17	2.6
$E\dot{n}_{exh}$ (kW)	0.07	0.10	0.14	0.21	0.26	0.03	0.08	0.09	0.12	0.15
$E\dot{n}_{loss}$ (kW)	9.56	8.16	10.51	14.38	16.15	8.13	6.95	7.25	7.594	9.45
η (%)	7.62	16.07	18.11	17.6	18.53	6.55	13.49	18.18	21.94	21.34
	P40G					**P80G**				
Load (Nm)	2	4	6	8	10	2	4	6	8	10
	Energy analysis					Energy analysis				
$E\dot{n}_{air}$ (kW)	0.81	0.91	1.223	1.51	1.79	0.91	1.11	1.33	1.62	1.69
$E\dot{n}_{fuel}$ (kW)	8.09	16.18	13.97	16.18	19.12	9.56	11.77	14.71	15.45	16.92
$E\dot{n}_{w}$ (kW)	0.79	1.58	2.35	3.11	3.74	0.79	1.57	2.34	3.01	3.23

$E\dot{n}_{exh}$ (kW)	0.10	0.11	0.15	0.21	0.28	0.11	0.14	0.17	0.23	0.27
$E\dot{n}_{loss}$ (kW)	8.00	15.4	12.68	14.36	16.88	9.56	11.17	13.52	13.82	15.11
η (%)	8.93	9.24	15.5	17.61	17.9	7.56	12.23	14.64	17.68	17.36
	P120G					**P95T5**				
Load (Nm)	2	4	6	8	10	2	4	6	8	10
	Energy analysis					Energy analysis				
$E\dot{n}_{air}$ (kW)	0.91	1.13	1.29	1.56	1.77	0.81	0.98	1.24	1.50	1.78
$E\dot{n}_{fuel}$ (kW)	12.51	11.78	13.98	14.72	18.4	9.52	8.79	11.73	13.19	14.66
$E\dot{n}_{w}$ (kW)	0.79	1.57	2.34	3.09	3.61	0.54	1.10	1.68	2.17	2.78
$E\dot{n}_{exh}$ (kW)	0.09	0.13	0.17	0.22	0.28	0.044	0.09	0.15	0.20	0.28
$E\dot{n}_{loss}$ (kW)	12.54	11.2	12.76	12.96	16.27	9.75	8.58	11.13	12.32	13.37
η (%)	5.90	12.2	15.37	19.03	17.93	5.25	11.29	13.01	14.79	16.91
	P90T10									
Load (Nm)	2	4	6	8	10					
	Energy analysis									
$E\dot{n}_{air}$ (kW)	0.81	0.97	1.22	1.45	1.71					
$E\dot{n}_{fuel}$ (kW)	10.23	10.23	12.42	16.07	15.34					
$E\dot{n}_{w}$ (kW)	0.54	1.09	1.67	2.22	2.62					
$E\dot{n}_{exh}$ (kW)	0.03	0.08	0.14	0.20	0.26					
$E\dot{n}_{loss}$ (kW)	10.47	10.02	11.83	15.1	14.17					
η (%)	4.91	9.76	12.25	12.68	15.37					

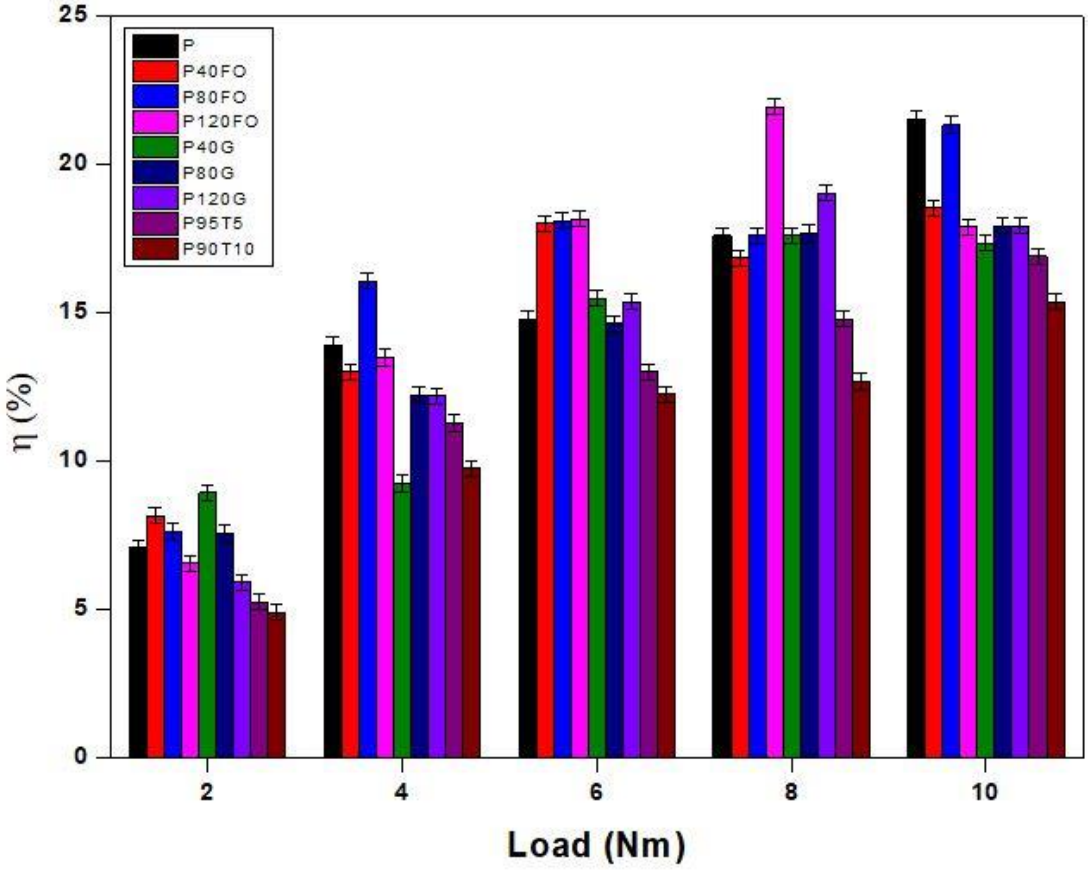

Figure 2: The energy efficiency for the testengine fuelled with the considered fuels.

4.2. Exergy analysis

Table 11 shows the exergy analysis results for the testengine running on the fuels considered in this analysis. The fuel exergy rates of all the fuel used in the analysis improved as the testengine load increased. For 2, 4, 6, 8, and 10 Nm, the fuel exergy rate of P40FO provided to the testengine was 9.40, 11.75, 12.54, 18.02, and 18.02 kW, respectively. This is because the amount of fuel consumption increased as the load of the testengine increased. The maximum exergy rates of fuel were recorded for neat petrol at a given load of testengine except for some concentrations of the graphite (G). As an outcome, the rates of fuel exergy at a load of 2 Nm were recorded to be 10.96, 9.40, 10.19, 8.62, 8.61, 10.18, 13.32, 10.15, and 10.89 kW for P, P40FO, P80FO, P120FO, P40G, P80G, P120G, P95T5, and P90T10, respectively.

For all the fuels considered in this analysis, the testengine's exergy loss rate increased as the engine's load increased. The exergy loss rates were recorded for P40FO (0.931 kW), P80FO (1.009

kW), P120FO (0.857 kW), P40G (0.841 kW), P80G (1.008 kW), P120G (1.32 kW), P95T5 (0.986 kW), and P90T10 (1.044 kW) at the load of testengine of 2 Nm. However, compared to other blends for the same testengine load of 2 Nm, the testengine's exergy loss rate for neat petrol (1.086 kW) was greater except for some graphite concentrations (G). For a 10 Nm load, the testengine's highest exergy loss rate was determined 2.23 kW for P80G, and it was then accompanied by P120G (2.156 kW).

The rate of exergy destruction enhanced as the testengine load increased. Except for some graphite concentrations (G), the maximum exergy destruction rates of the testengine were recorded for the petrol engine at applied load. The rates of exergy destruction of the testengine were determined to be 8.99 kW for P40FO, 8.37 kW for P80FO, 7.19 kW for P120FO, 6.95 kW for P40G, 8.35 kW for P80G, 11.18 kW for P120G, 8.60 kW for P95T5, and 9.29 kW for P90T10 at a load of 2 Nm. At this testengine load, the exergy destruction rate of the testengine for petrol fuel was 9.06 kW. At a testengine load of 10 Nm, the maximum exergy destruction rate was 14.31 kW for P40G fuel in this analysis.

The rates of exergy fuel, exergy loss, and exergy destruction of graphite-blended fuels are greater. This is due to their high thermal conductivity [43], and inside the combustion chamber, graphite nanoparticles serve as heat sinks for contiguous fuel droplets, speeding up the vaporization process. Therefore, once the petrol is converted to vapors, nanoparticles are carried away from the droplets, allowing for faster preparation of combustible fusions. These features help to enhance the combustion process inside the cylinder, resulting in a rise in exergy fuel, exergy loss, and exergy destruction rates.

Figure 3 depicts the testengine's exergy performance variation as a function of the testengine load for the fuels prepared in this analysis. The testengine's exergy efficiency improved as the load on the engine increased. The testengine's maximum exergy efficiency was found to be 23.05% for P120FO petrol, at a load of 8 Nm. Higher exergy efficiencies for P120FO blends may be attributed to lower fuel consumption requirements.

Previous studies have also shown that iron oxide (Fe_2O_3) reduces fuel consumption [45]. The additional dissolved oxygen decreased kinematic viscosity of the fuel droplets influence combustion and ultimately consumption of fuel. In the intermolecular spaces of the fuel droplets, iron oxide nanoparticles are suspended and dispersed can reduce the kinematic viscosity, allowing adjacent layers to slip more efficiently, as shown in **Table 3.** This can result in more accurate fuel spraying and increased air-fuel mixing, resulting in full combustion and better fuel usage. Another study backs up this argument [46] that reduced fuel viscosity improves atomization and increases mixing rate, affecting the fuel injection.

Table 11: The exergy analysis results for the testengine fuelled with the considered fuels.

	P					**P40FO**				
Load (Nm)	2	4	6	8	10	2	4	6	8	10
	Exergy analysis					Exergy analysis				
$E\dot{x}_{air} \times 10^{-3}$ (kW)	0.53	0.81	1.16	1.57	2.00	0.61	0.94	1.19	1.63	2
$E\dot{x}_{fuel}$ (kW)	10.96	10.96	15.66	17.22	17.22	9.403	11.75	12.54	18.02	18.02
$E\dot{x}_{w}$ (kW)	0.79	1.58	2.35	3.11	3.86	0.79	1.57	2.35	3.11	3.59
$E\dot{x}_{exh}$ (kW)	0.017	0.045	0.056	0.057	0.080	0.020	0.032	0.045	0.062	0.083
$E\dot{x}_{loss}$ (kW)	1.08	1.06	1.59	1.83	1.79	0.93	1.15	1.26	1.94	1.95
$E\dot{x}_{dest}$ (kW)	9.06	8.27	11.65	12.22	11.49	7.65	8.99	8.87	12.9	12.39
ψ (%)	7.24	14.43	15.05	18.11	22.43	8.441	13.42	18.78	17.26	19.92
	P80FO					**P120FO**				
Load (Nm)	2	4	6	8	10	2	4	6	8	10

	Exergy analysis					Exergy analysis				
$E\dot{x}_{air} \times 10^{-3}$ (kW)	0.62	0.84	1.22	1.68	2.12	0.80	0.92	1.07	1.30	1.45
$E\dot{x}_{fuel}$ (kW)	10.19	9.40	12.54	17.25	19.6	8.62	7.84	8.62	9.41	11.77
$E\dot{x}_{w}$ (kW)	0.79	1.58	2.35	3.11	3.73	0.57	1.09	1.63	2.17	2.60
$E\dot{x}_{exh}$ (kW)	0.015	0.023	0.038	0.058	0.074	0.008	0.020	0.024	0.031	0.039
$E\dot{x}_{loss}$ (kW)	1.009	0.91	1.25	1.85	2.13	0.85	0.77	0.86	0.97	1.25
$E\dot{x}_{dest}$ (kW)	8.37	6.89	8.89	12.23	13.66	7.19	5.94	6.10	6.23	7.86
ψ (%)	7.80	16.81	18.8	18.07	19.04	6.64	13.99	18.93	23.05	22.16
	P40G					**P80G**				
Load (Nm)	2	4	6	8	10	2	4	6	8	10
	Exergy analysis					Exergy analysis				
$E\dot{x}_{air} \times 10^{-3}$ (kW)	1.15	1.25	1.73	2.35	2.91	1.24	1.62	1.89	2.28	2.60
$E\dot{x}_{fuel}$ (kW)	8.61	17.23	14.88	17.23	20.36	10.18	12.59	15.67	16.45	18.02
$E\dot{x}_{w}$ (kW)	0.79	1.58	2.35	3.11	3.74	0.79	1.57	2.34	3.01	3.23
$E\dot{x}_{exh}$ (kW)	0.026	0.027	0.039	0.056	0.077	0.031	0.038	0.048	0.065	0.083
$E\dot{x}_{loss}$ (kW)	0.84	1.70	1.51	1.83	2.23	1.00	1.24	1.62	1.77	2.02

$E\dot{x}_{dest}$ (kW)	6.95	13.92	10.97	12.23	14.31	8.35	9.67	11.67	11.6	12.68
ψ (%)	9.23	9.16	15.82	18.08	18.38	7.78	12.58	14.99	18.34	17.93
	P120G					**P95T5**				
Load (Nm)	2	4	6	8	10	2	4	6	8	10
	Exergy analysis					Exergy analysis				
$E\dot{x}_{air} \times 10^{-3}$ (kW)	0.58	0.86	1.15	1.51	1.79	0.18	0.37	0.50	0.64	0.89
$E\dot{x}_{fuel}$ (kW)	13.32	12.54	14.89	15.68	19.6	10.15	9.36	12.49	14.05	15.61
$E\dot{x}_{w}$ (kW)	0.79	1.57	2.34	3.09	3.61	0.54	1.10	1.68	2.17	2.78
$E\dot{x}_{exh}$ (kW)	0.021	0.033	0.047	0.062	0.082	0.007	0.021	0.038	0.055	0.083
$E\dot{x}_{loss}$ (kW)	1.32	1.26	1.53	1.68	2.15	0.98	0.90	1.24	1.46	1.65
$E\dot{x}_{dest}$ (kW)	11.18	9.67	10.97	10.84	13.74	8.60	7.33	9.51	10.35	11.09
ψ (%)	5.95	12.56	15.77	19.76	18.46	5.35	11.79	13.51	15.47	17.81
	P90T10									
	2	4	6	8	10					
	Exergy analysis									
$E\dot{x}_{air} \times 10^{-3}$ (kW)	0.17	0.32	0.50	0.74	1.08					
$E\dot{x}_{fuel}$ (kW)	10.89	10.89	13.23	17.12	16.34					

$E\dot{x}_w$ (kW)	0.54	1.09	1.67	2.22	2.62
$E\dot{x}_{exh}$ (kW)	0.005	0.018	0.037	0.053	0.072
$E\dot{x}_{loss}$ (kW)	1.04	1.08	1.34	1.80	1.82
$E\dot{x}_{dest}$ (kW)	9.29	8.69	10.18	13.04	11.82
ψ (%)	4.98	10.04	12.64	12.98	16.04

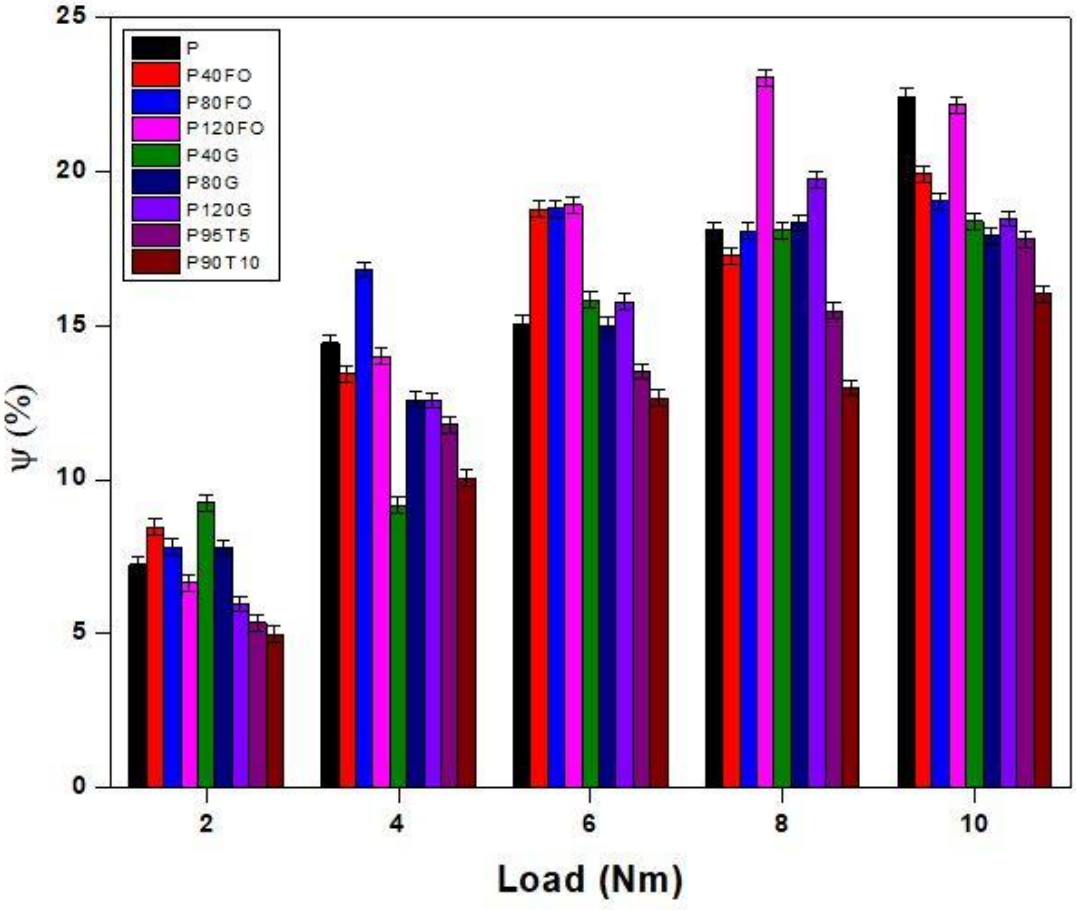

Figure 3: The exergy efficiency for the testengine fuelled with the considered fuels.

4.3. Thermoeconomic analysis

The cost of the system's capital investment was calculated as $20,000. **Table 12** summarizes the testengine's thermoeconomic research results on the fuels investigated in this report.

For all fuels included in this study, the testengine's R_{en} value improved as the testengine load increased, as shown in **Table 12**. P120FO and P120G had the minimum and maximum R_{en} values of the testengine, respectively.

The testengine's $R_{ex:loss}$ values increased as the load on the engine increased. Except for certain graphite (G) concentrations, the testengine had the maximum $R_{ex:loss}$ value for petrol fuel relative to other blends at the same load on the testengine. P120FO had the lowest $R_{ex:loss}$ value at 4 Nm, while P40G had the highest at 10 Nm.

With the increasing load on the testengine, the $R_{ex:dest}$ values of the testengine improved. Except for certain graphite (G) concentrations, the highest $R_{ex:dest}$ values of the testengine were recorded for petrol engines at all testengine loads. The maximum $R_{ex:dest}$ value was obtained for P40G at a load of 4 Nm on testengine. The testengine had the lowest $R_{ex:dest}$ values for P120FO of all the loads considered.

Table 12: The thermoeconomic analysis results for the testengine fuelled with the considered fuels.

	P					**P40FO**				
Load (Nm)	2	4	6	8	10	2	4	6	8	10
	Thermoeconomic analysis					Thermoeconomic analysis				
$R_{en} \times 10^{-3}$ (kW/$)	0.51	0.47	0.66	0.71	0.69	0.44	0.52	0.527	0.75	0.74
$R_{ex,loss} \times 10^{-3}$ (kW/$)	0.054	0.053	0.079	0.091	0.089	0.046	0.057	0.063	0.0973	0.0978
$R_{ex,dest} \times 10^{-3}$ (kW/$)	0.45	0.41	0.58	0.61	0.57	0.38	0.44	0.443	0.645	0.619

	P80FO					**P120FO**				
Load (Nm)	2	4	6	8	10	2	4	6	8	10
	Thermoeconomic analysis					Thermoeconomic analysis				
$R_{en} \times 10^{-3}$ (kW/$)	0.478	0.408	0.525	0.719	0.807	0.406	0.347	0.362	0.379	0.472
$R_{ex,loss} \times 10^{-3}$ (kW/$)	0.05	0.045	0.062	0.092	0.106	0.042	0.038	0.043	0.048	0.062
$R_{ex,dest} \times 10^{-3}$ (kW/$)	0.418	0.344	0.444	0.611	0.682	0.359	0.297	0.305	0.311	0.393
	P40G					**P80G**				
Load (Nm)	2	4	6	8	10	2	4	6	8	10
	Thermoeconomic analysis					Thermoeconomic analysis				
$R_{en} \times 10^{-3}$ (kW/$)	0.400	0.769	0.634	0.717	0.844	0.478	0.558	0.676	0.691	0.755
$R_{ex,loss} \times 10^{-3}$ (kW/$)	0.042	0.089	0.075	0.091	0.111	0.050	0.062	0.081	0.088	0.101
$R_{ex,dest} \times 10^{-3}$ (kW/$)	0.347	0.696	0.548	0.611	0.715	0.417	0.483	0.582	0.579	0.634
	P120G					**P95T5**				
Load (Nm)	2	4	6	8	10	2	4	6	8	10
	Thermoeconomic analysis					Thermoeconomic analysis				
$R_{en} \times 10^{-3}$ (kW/$)	0.627	0.56	0.637	0.647	0.813	0.487	0.429	0.55	0.616	0.668

$R_{ex,loss} \times 10^{-3}$ (kW/$)	0.066	0.062	0.076	0.084	0.107	0.049	0.045	0.062	0.073	0.082
$R_{ex,dest} \times 10^{-3}$ (kW/$)	0.559	0.483	0.548	0.541	0.687	0.430	0.366	0.479	0.517	0.554

	P90T10				
Load (Nm)	2	4	6	8	10
	Thermoeconomic analysis				
$R_{en} \times 10^{-3}$ (kW/$)	0.523	0.500	0.591	0.754	0.708
$R_{ex,loss} \times 10^{-3}$ (kW/$)	0.052	0.054	0.067	0.090	0.091
$R_{ex,dest} \times 10^{-3}$ (kW/$)	0.464	0.43	0.508	0.651	0.591

4.4. Sustainability analysis

The testengine's improvement potential varies with the testengine load for the fuels considered in this study, as shown in **Figure 4**.

As shown in **Figure 4,** the testengine's improvement potential increased as the testengine load increased for all considered fuels. When the testengine had been fuelled with P120FO, the lowest improvement potential values were observed. This is because P120FO had lower irreversibility. Graphite-blended fuels had the highest improvement potential values in all testengine loads, followed by petrol and TPO-blended fuels. When the testengine had been fuelled with petrol, graphite-blended, and TPO-blended fuel, there was more irreversibility to prevent as compared to the blends of Fe_2O_3.

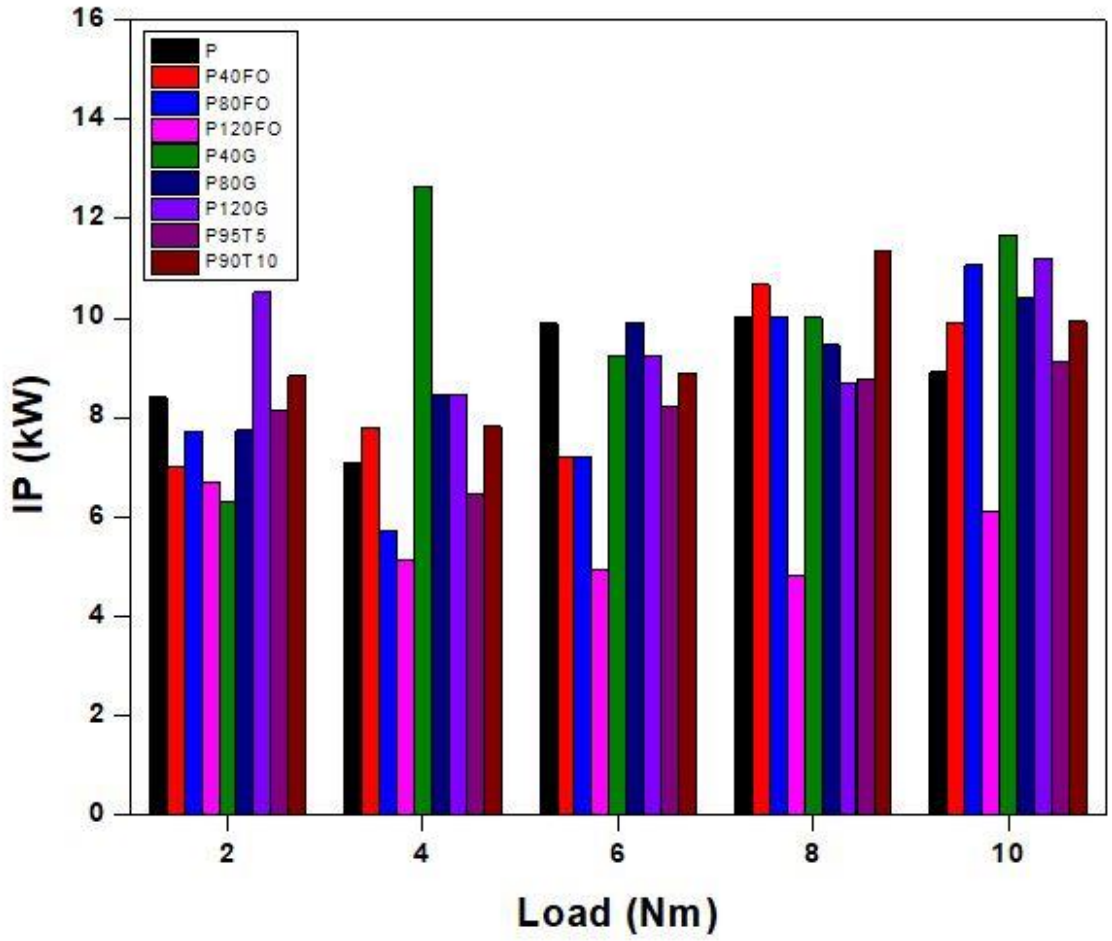

Figure 4: The improvement potential for the testengine fuelled with the considered fuels.

Figure 5 illustrates the change of the depletion number of testengine with load for the considered fuels for the analysis. With the increasing load on the testengine, the depletion number of the testengine decreased slightly. P120FO had the lowest depletion number values. Petrol, graphite-blended, and TPO-blended fuels, on the other hand, had almost the maximum values of depletion number for all testengine loads.

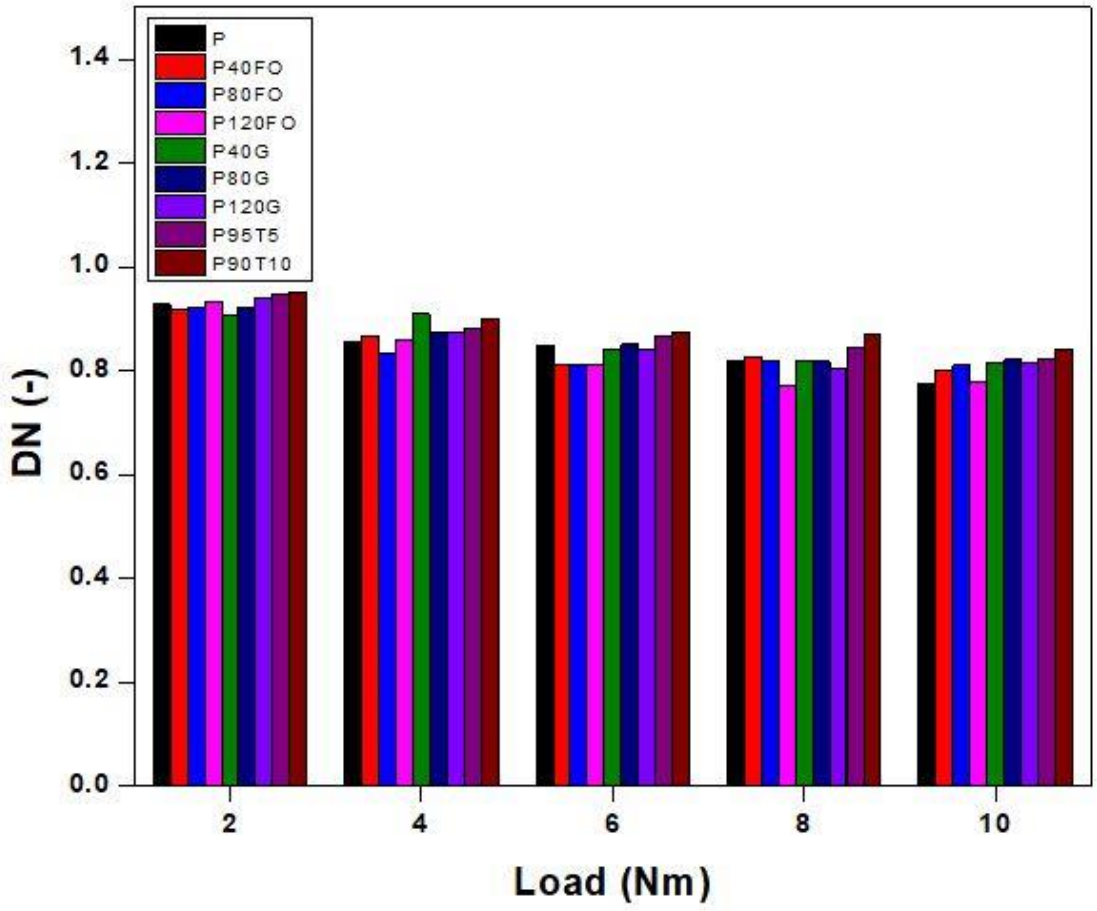

Figure 5: The depletion number for the testengine fuelled with the considered fuels.

The variation of the testengine's sustainability index with the load for the fuels considered in this study is depicted in **Figure 6**. The testengine's sustainability index increased as the testengine load increased. In all testengine loads, P120FO had the highest sustainability index. In all testengine loads, petrol, graphite-blended, and TPO-blended fuels had the lowest sustainability index. Compared to the other fuels considered in this analysis, the outcomes indicate that P120FO was the most sustainable.

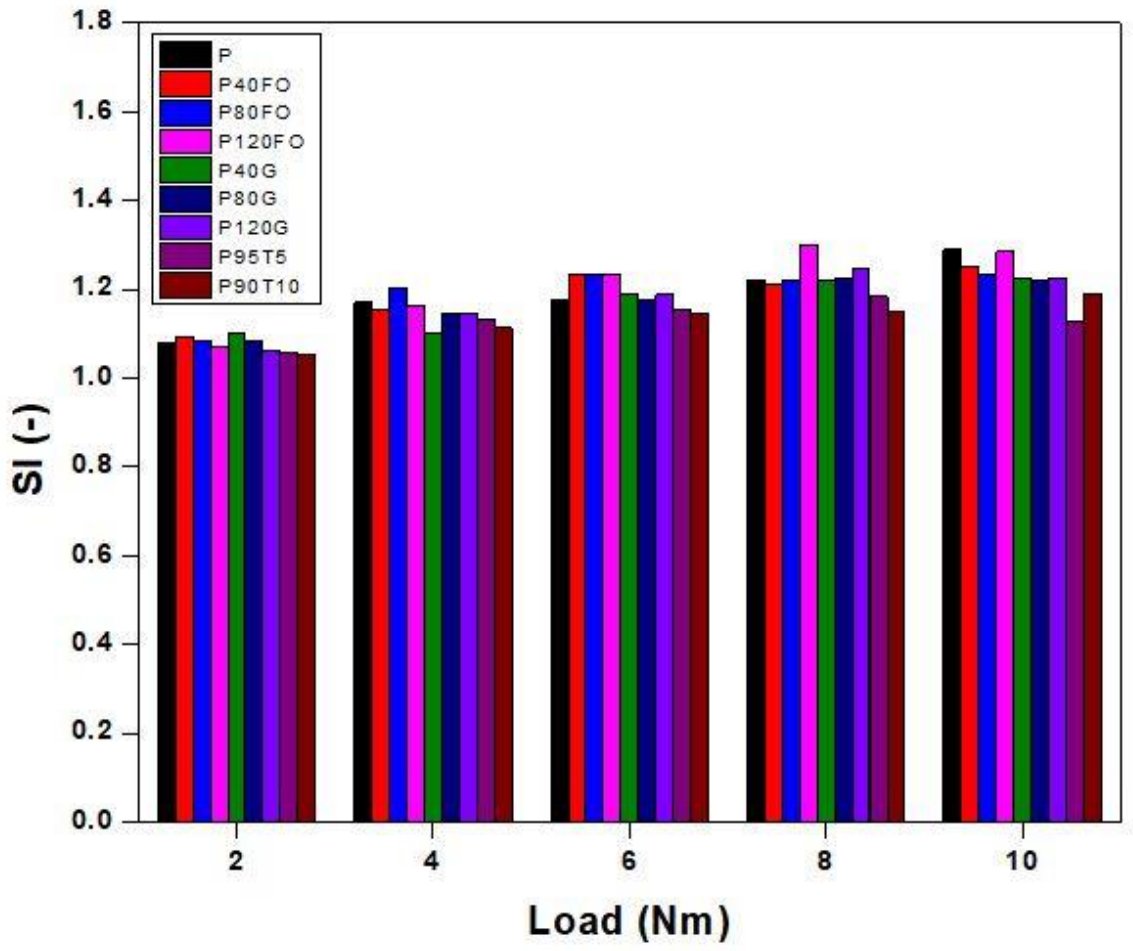

Figure 6: The sustainability index for the testengine fuelled with the considered fuels.

According to the findings, the best engine performance in terms of energy, exergy, economic, and sustainability was obtained when the testengine was fuelled with P120FO. **Table 13** shows the sustainability analysis for the testengine fuelled with the different fuels.

Table 13: The sustainability analysis results for the testengine fuelled with the considered fuels.

	P					**P40FO**				
Load (Nm)	2	4	6	8	10	2	4	6	8	10
	Sustainability analysis					Sustainability analysis				
IP (kW)	8.40	7.08	9.89	10.01	8.91	7.011	7.78	7.21	10.67	9.92
DN	0.92	0.855	0.849	0.818	0.775	0.915	0.865	0.812	0.827	0.80
SI	1.078	1.169	1.177	1.221	1.289	1.092	1.155	1.231	1.209	1.249
	P80FO					**P120FO**				

Load (Nm)	2	4	6	8	10	2	4	6	8	10
	Sustainability analysis					Sustainability analysis				
IP (kW)	7.72	5.73	7.22	10.02	11.06	6.71	5.11	4.94	4.79	6.12
DN	0.92	0.83	0.81	0.819	0.809	0.933	0.86	0.81	0.76	0.77
SI	1.08	1.20	1.23	1.22	1.23	1.07	1.16	1.23	1.3	1.28
	P40G					**P80G**				
Load (Nm)	2	4	6	8	10	2	4	6	8	10
	Sustainability analysis					Sustainability analysis				
IP (kW)	6.31	12.65	9.23	10.01	11.68	7.74	8.45	9.90	9.46	10.41
DN	0.907	0.908	0.841	0.819	0.816	0.922	0.874	0.850	0.816	0.820
SI	1.102	1.101	1.188	1.221	1.225	1.084	1.144	1.176	1.225	1.218
	P120G					**P95T5**				
Load (Nm)	2	4	6	8	10	2	4	6	8	10
	Sustainability analysis					Sustainability analysis				
IP (kW)	10.52	8.459	9.23	8.69	11.21	8.14	6.46	8.23	8.74	9.11
DN	0.940	0.874	0.842	0.802	0.815	0.946	0.882	0.864	0.845	0.821
SI	1.06	1.14	1.18	1.24	1.22	1.05	1.13	1.15	1.18	1.21
	P90T10									
Load (Nm)	2	4	6	8	10					
	Sustainability analysis									
IP (kW)	8.83	7.81	8.89	11.35	9.92					
DN	0.95	0.899	0.873	0.870	0.839					
SI	1.05	1.11	1.145	1.149	1.191					

5. Conclusion

The energy, exergy, sustainability, and economic assessments were executed on 1-cylinder, four-stroke, air-cooled, SI engine fuelled with neat petrol, Fe_2O_3-petrol, graphite-petrol, and TPO-

petrol blended fuels having various volumetric fractions at the engine loads of 2 to 10 Nm with an increment of 2 Nm and constant speed of 3500 rpm.

The following are the study's key conclusions:

- When the testengine was fuelled with P120FO, it had the highest energy efficiency for almost all the testengine load.
- At almost all loads on the testengine, P120FO had the highest exergy efficiency.
- In general, lower values of R_{en}, $R_{ex:loss,}$ and $R_{ex:dest}$ were recorded for P120FO when matched with neat petrol fuel. This indicates that in terms of thermoeconomic, P120FO had better performance.
- The P120FO had the maximum sustainability index for all the testengine loads, while the petrol fuel had the lowest. Fe_2O_3-petrol blends are more sustainable than neat petrol, according to these findings.
- The higher the graphite content in graphite-petrol blends, the poorer the testengine efficiency in terms of exergy, energy, sustainability, and economics, but at lower engine loads, the performance was comparable to that of petrol fuel.
- Almost the same trend was shown by TPO-petrol blended fuels as that of graphite-petrol blends.

Without requiring any modifications, P120FO can be used as a fuel additive for spark-ignition engines because of its exceptional energy and exergy, thermoeconomic, and sustainability index properties. P120FO as a fuel in SI engines allows for environmental protection, energy recovery, and reuse of limited fossil fuel supplies.

Acknowledgments

The authors acknowledge the support provided by Khwaja Fareed University of Engineering and Information Technology (KFUEIT), Rahim Yar Khan, and Universiti Sains Malaysia (USM). Also acknowledged the support provided by Mr. Muhammad Zeeshan and Mr. Muhammad Tayyab for facilitating the laboratory work. The authors are also grateful for the financial support from the

Ministry of Higher Education (MOHE) of Malaysia under the Fundamental Research Grant Scheme (FRGS) [203.PMEKANIK.6071444] and Universiti Sains Malaysia. This work was also supported by Taif University researchers supporting project number (TURSP–2020/40), Taif University, Taif, Saudi Arabia.

Nomenclature

▲	increasing value
▼	decreasing value
C_p	specific heat capacity (kJ/kg. K)
CH_3OH	methyl alcohol
CO	carbon monoxide
CO_2	carbon dioxide
ex	specific exergy rate (kJ/kg)
$\dot{E}$	energy rate (kW)
Fe_2O_3	ferric oxide (FO) or iron oxide
h	specific enthalpy (kJ/kg)
H_u	calorific value or lower heating value (kJ/kg)
K	cost ($)
$\dot{m}$	mass flow rate (kg/s)
n	crankshaft speed (rpm)
N	nitrogen
NO or NO_x	oxides of nitrogen
O_2	oxygen
P	pressure (kPa)
R	thermoeconomic parameter (kW/$)
$\overline{R}$	general gas constant (kJ/kmolK)

SO_2	sulfur dioxide
T	temperature (K) and torque (Nm)
$\dot{V}$	volumetric flow rate (m^3/s)
y	molar fraction (%)

Greek Symbol

ε	chemical exergy factor (-)
ρ	density (kg/m^3)
η_v	volumetric efficiency (%)
η_m	mechanical efficiency (%)
η	energy efficiency (%)
ψ	exergy efficiency (%)
ω	angular velocity (rad/s)

Abbreviations

A/F	air to fuel ratio
BSFC	brake specific fuel consumption
BP	brake power
BTE	brake thermal efficiency
DN	depletion Number
EXCEM	exergy cost energy mass method
FC	fuel Consumption
G	graphite
HC	hydrocarbons
IP	improvement potential (kW)
P	neat petrol

P40FO	Petrol + 40 mg/liter Fe_2O_3
P80FO	Petrol + 80 mg/liter Fe_2O_3
P120FO	Petrol + 120 mg/liter Fe_2O_3
P40G	Petrol + 40 mg/liter Graphite
P80G	Petrol + 80 mg/liter Graphite
P120G	Petrol + 120 mg/liter Graphite
P95T5	95% Petrol + 5% Tire Pyrolysis Oil
P90T10	90% Petrol + 10% Tire Pyrolysis Oil
PM	particulate matter
SI	sustainability index and spark ignition
TPO	Tire Pyrolysis Oil
UHC	unburned hydrocarbons

Subscripts

air	air
cap	capital
dest	destruction
en	energy
ex	exergy
exh	exhaust
gen	generation
in	inlet
Out	outlet
OCC	other
O-M	operation & maintenance
W	work
O	environmental state

References

[1] Gürbüz H, Akçay İH. Evaluating the effects of boosting intake-air pressure on the performance and environmental-economic indicators in a hydrogen-fueled SI engine. International Journal of Hydrogen Energy 2021;46:28801–10. doi:https://doi.org/10.1016/j.ijhydene.2021.06.099.

[2] Akal D, Öztuna S, Büyükakın MK. A review of hydrogen usage in internal combustion engines (gasoline-Lpg-diesel) from combustion performance aspect. International Journal of Hydrogen Energy 2020;45:35257–68. doi:https://doi.org/10.1016/j.ijhydene.2020.02.001.

[3] El-Seesy AI, Nour M, Attia AMA, He Z, Hassan H. Investigation the effect of adding graphene oxide into diesel/higher alcohols blends on a diesel engine performance. International Journal of Green Energy 2020;17:233–53. doi:10.1080/15435075.2020.1722132.

[4] Duc PM, Wattanavichien K. Study on biogas premixed charge diesel dual fuelled engine. Energy Conversion and Management 2007;48:2286–308. doi:10.1016/j.enconman.2007.03.020.

[5] Demirbas A. Progress and recent trends in biofuels. Progress in Energy and Combustion Science 2007;33:1–18. doi:10.1016/j.pecs.2006.06.001.

[6] Elliott DC. Historical Developments in Hydroprocessing Bio-oils. Energy & Fuels 2007;21:1792–815. doi:10.1021/ef070044u.

[7] Mohan D, Pittman CU, Steele PH. Pyrolysis of Wood/Biomass for Bio-oil: A Critical Review. Energy & Fuels 2006;20:848–89. doi:10.1021/ef0502397.

[8] Mehri B, Pirouzfar V, Bagheri S, Pedram MZ. Modelling and optimization of exhaust pollutants and the properties and characteristics of ethanol-diesel through a statistical approach. The Canadian Journal of Chemical Engineering 2017;95:1054–62. doi:https://doi.org/10.1002/cjce.22765.

[9] Koç M, Sekmen Y, Topgül T, Yücesu HS. The effects of ethanol–unleaded gasoline blends

on engine performance and exhaust emissions in a spark-ignition engine. Renewable Energy 2009;34:2101–6. doi:https://doi.org/10.1016/j.renene.2009.01.018.

[10] Man H, Liu H, Xiao Q, Deng F, Yu Q, Wang K, et al. How ethanol and gasoline formula changes evaporative emissions of the vehicles. Applied Energy 2018;222:584–94. doi:https://doi.org/10.1016/j.apenergy.2018.03.109.

[11] Elfasakhany A. Investigations on the effects of ethanol–methanol–gasoline blends in a spark-ignition engine: Performance and emissions analysis. Engineering Science and Technology, an International Journal 2015;18:713–9. doi:https://doi.org/10.1016/j.jestch.2015.05.003.

[12] Al-Hasan M. Effect of ethanol–unleaded gasoline blends on engine performance and exhaust emission. Energy Conversion and Management 2003;44:1547–61. doi:https://doi.org/10.1016/S0196-8904(02)00166-8.

[13] Hsieh W-D, Chen R-H, Wu T-L, Lin T-H. Engine performance and pollutant emission of an SI engine using ethanol–gasoline blended fuels. Atmospheric Environment 2002;36:403–10. doi:https://doi.org/10.1016/S1352-2310(01)00508-8.

[14] Yanju W, Shenghua L, Hongsong L, Rui Y, Jie L, Ying W. Effects of Methanol/Gasoline Blends on a Spark Ignition Engine Performance and Emissions. Energy & Fuels 2008;22:1254–9. doi:10.1021/ef7003706.

[15] Karagöz M, Ağbulut Ü, Sarıdemir S. Waste to energy: Production of waste tire pyrolysis oil and comprehensive analysis of its usability in diesel engines. Fuel 2020;275. doi:10.1016/j.fuel.2020.117844.

[16] Hasan A, Dincer I. Assessment of an Integrated Gasification Combined Cycle using waste tires for hydrogen and fresh water production. International Journal of Hydrogen Energy 2019;44:19730–41. doi:https://doi.org/10.1016/j.ijhydene.2019.05.075.

[17] Hatami M, Hasanpour M, Jing D. Recent developments of nanoparticles additives to the consumables liquids in internal combustion engines: Part I: Nano-fuels. Journal of Molecular Liquids 2020;318. doi:10.1016/j.molliq.2020.114250.

[18] Chan JH, Tsolakis A, Herreros JM, Kallis KX, Hergueta C, Sittichompoo S, et al. Combustion, gaseous emissions and PM characteristics of Di-Methyl Carbonate (DMC)-gasoline blend on gasoline Direct Injection (GDI) engine. Fuel 2020;263:116742. doi:https://doi.org/10.1016/j.fuel.2019.116742.

[19] Valihesari M, Pirouzfar V, Ommi F, Zamankhan F. Investigating the effect of Fe2O3 and TiO2 nanoparticle and engine variables on the gasoline engine performance through statistical analysis. Fuel 2019;254:115618. doi:https://doi.org/10.1016/j.fuel.2019.115618.

[20] Oh SH, Yoon SH, Song H, Han JG, Kim J-M. Effect of hydrogen nanobubble addition on combustion characteristics of gasoline engine. International Journal of Hydrogen Energy 2013;38:14849–53. doi:https://doi.org/10.1016/j.ijhydene.2013.09.063.

[21] Amirabedi M, Jafarmadar S, Khalilarya S. Experimental investigation the effect of Mn2O3 nanoparticle on the performance and emission of SI gasoline fueled with mixture of ethanol and gasoline. Applied Thermal Engineering 2019;149:512–9. doi:https://doi.org/10.1016/j.applthermaleng.2018.12.058.

[22] Ali MKA, Fuming P, Younus HA, Abdelkareem MAA, Essa FA, Elagouz A, et al. Fuel economy in gasoline engines using Al2O3/TiO2 nanomaterials as nanolubricant additives. Applied Energy 2018;211:461–78. doi:https://doi.org/10.1016/j.apenergy.2017.11.013.

[23] Taghavifar H, Kaleji BK, Kheyrollahi J. Application of composite TNA nanoparticle with bio-ethanol blend on gasoline fueled SI engine at different lambda ratios. Fuel 2020;277. doi:10.1016/j.fuel.2020.118218.

[24] Sayin C, Hosoz M, Canakci M, Kilicaslan I. Energy and exergy analyses of a gasoline engine. International Journal of Energy Research 2007;31:259–73. doi:https://doi.org/10.1002/er.1246.

[25] Ghazikhani M, Hatami M, Safari B. The effect of alcoholic fuel additives on exergy parameters and emissions in a two stroke gasoline engine. Arabian Journal for Science and Engineering 2012;39:2117–25. doi:10.1007/s13369-013-0738-3.

[26] Alasfour FN. Butanol—A single-cylinder engine study: availability analysis. Applied Thermal Engineering 1997;17:537–49. doi:https://doi.org/10.1016/S1359-4311(96)00069-5.

[27] Sezer İ, Bilgin A. Mathematical analysis of spark ignition engine operation via the combination of the first and second laws of thermodynamics. Proceedings of the Royal Society A: Mathematical, Physical and Engineering Sciences 2008;464:3107–28. doi:10.1098/rspa.2008.0190.

[28] Mithaiwal KA, Modi AJ, Gosai DC. Energy and Exergy Analysis on Si Engine by Blend of Ethanol with Petrol. International Journal of Advanced Engineering Research and Science 2017;4:49–61. doi:10.22161/ijaers.4.4.6.

[29] Özcan H, Çakmak A. Comparative Exergy Analysis of Fuel Additives Containing Oxygen and HC based in a Spark-Ignition (SI) engine. International Journal of Automotive Engineering and Technologies 2018;7:124–33. doi:10.18245/ijaet.486410.

[30] Karagoz M, Uysal C, Agbulut U, Saridemir S. Energy, exergy, economic and sustainability assessments of a compression ignition diesel engine fueled with tire pyrolytic oil−diesel blends. Journal of Cleaner Production 2020;264:121724. doi:10.1016/j.jclepro.2020.121724.

[31] Dogan B, Yf_ilyurt M, Erol D, Akmak A. A Study Toward Analyzing the Energy, Exergy and Sustainability Index Based on Performance and Exhaust Emission Characteristics of a Spark-Ignition Engine Fuelled with the Binary Blends of Gasoline and Methanol or Ethanol. Environmental Science, 2020, p. 529–48. doi:10.29137/umagd.728802.

[32] Sezer İ, Altin İ, Bilgin A. Exergetic Analysis of Using Oxygenated Fuels in Spark-Ignition (SI) Engines. Energy & Fuels 2009;23:1801–7. doi:10.1021/ef8002608.

[33] Zhu Y, Murali S, Cai W, Li X, Suk JW, Potts JR, et al. Graphene and Graphene Oxide: Synthesis, Properties, and Applications. Advanced Materials 2010;22:3906–24. doi:https://doi.org/10.1002/adma.201001068.

[34] Sun W, Cao L, Deng Y, Gong S, Shi F, Li G, et al. Direct electrochemistry with enhanced electrocatalytic activity of hemoglobin in hybrid modified electrodes composed of graphene

and multi-walled carbon nanotubes. Analytica Chimica Acta 2013;781:41–7. doi:https://doi.org/10.1016/j.aca.2013.04.010.

[35] Sarıdemir S, Ağbulut Ü. Combustion, performance, vibration and noise characteristics of cottonseed methyl ester–diesel blends fuelled engine. Biofuels 2019;0:1–10. doi:10.1080/17597269.2019.1667658.

[36] Caliskan H, Mori K. Thermodynamic, environmental and economic effects of diesel and biodiesel fuels on exhaust emissions and nano-particles of a diesel engine. Transportation Research Part D: Transport and Environment 2017;56:203–21. doi:10.1016/j.trd.2017.08.009.

[37] Kotas TJ. The Exergy Method of Thermal Plant Analysis. 1985.

[38] Adrian Bejan, George Tsatsaronis MJM. Thermal Design and Optimization. 1996.

[39] Rosen MA, Dincer I. Exergy–cost–energy–mass analysis of thermal systems and processes. Energy Conversion and Management 2003;44:1633–51. doi:https://doi.org/10.1016/S0196-8904(02)00179-6.

[40] Rosen MA, Dincer I, Kanoglu M. Role of exergy in increasing efficiency and sustainability and reducing environmental impact. Energy Policy 2008;36:128–37. doi:10.1016/j.enpol.2007.09.006.

[41] Van Gool W. Energy Policy: Fairy Tales and Factualities BT - Innovation and Technology — Strategies and Policies. Innovation and Technology — Strategies and Policies, 1997, p. 93–105.

[42] Connelly L, Koshland CP. Two aspects of consumption: Using an exergy-based measure of degradation to advance the theory and implementation of industrial ecology. Resources, Conservation and Recycling 1997;19:199–217. doi:10.1016/S0921-3449(96)01180-9.

[43] Fugallo G, Cepellotti A, Paulatto L, Lazzeri M, Marzari N, Mauri F. Thermal Conductivity of Graphene and Graphite: Collective Excitations and Mean Free Paths. Nano Letters 2014;14:6109–14. doi:10.1021/nl502059f.

[44] Shan X, Que L. High-valent nonheme iron-oxo species in biomimetic oxidations. Journal of Inorganic Biochemistry 2006;100:421–33. doi:https://doi.org/10.1016/j.jinorgbio.2006.01.014.

[45] Zhu M, Ma Y, Zhang D. Effect of a homogeneous combustion catalyst on the combustion characteristics and fuel efficiency in a diesel engine. Applied Energy 2012;91:166–72. doi:https://doi.org/10.1016/j.apenergy.2011.09.007.

[46] Doğan O, Çelik MB, Özdalyan B. The effect of tire derived fuel/diesel fuel blends utilization on diesel engine performance and emissions. Fuel 2012;95:340–6. doi:https://doi.org/10.1016/j.fuel.2011.12.033.